Title:

The pathology of aging 129S6/SvEvTac mice

Authors:

Enrico Radaelli, Vittoria Castiglioni, Camilla Recordati, Alberto Gobbi, Manuela Capillo, Anna Invernizzi, Eugenio Scanziani, Francesco Marchesi

Affiliations:

VIB11 Center for the Biology of Disease, KU Leuven Center for Human Genetics, Leuven, Belgium (ER)

InfraMouse, KU Leuven-VIB, Leuven, Belgium (ER)

Mouse and Animal Pathology Laboratory, Filarete Foundation, Milan, Italy (VC, CR, ES)

COGENTECH S.C.A.R.L., Milan, Italy (MC, AG)

Department of Experimental Oncology, European Institute of Oncology, Milan, Italy (MC, AG)

Istituto Zooprofilattico Sperimentale della Lombardia e dell'Emila Romagna, Sezione di Milano, Milan, Italy (AI)

Department of Veterinary Sciences and Public health, University of Milan, Milan, Italy (ES)

School of Veterinary Medicine, College of Medical Veterinary and Life Sciences, University of Glasgow, Glasgow, Scotland, United Kingdom (FM)

Abstract:

The 129 mouse strain is commonly used for the generation of genetically engineered mice (GEM). Genetic drift or accidental contamination during outcrossing has resulted in several 129 substrains. Comprehensive data on the spontaneous age-related pathology exist for the 129S4/SvJae substrain, whereas only limited information is available on the disease spectrum of other 129 sublines. This longitudinal aging study describes the lifespan and spontaneous lesions of 44 male and 18 female mice belonging to the 129S6/SvEvTac substrain. Median survival time was 778 and 770 days for males and females, respectively. Tumors of lung and Harderian gland were the most common neoplasms in both sexes. Hepatocellular tumors occurred mainly in males. Hematopoietic tumors were observed at low frequency. Suppurative and ulcerative blepharoconjunctivitis emerged as the most common nonneoplastic condition in both sexes. Corynebacterial species (primarely *C. urealyticum* and *C. pseudodiphtheriticum*) were isolated from animals affected by blepharoconjunctivitis and in some cases from unaffected mice. A clear causal association between *Corynebacterium* spp. infection and blepharoconjunctivitis could not be inferred. Polyarteritis occurred only in males and was identified as the most common non-neoplastic contributory cause of death. Eosinophilic crystalline pneumonia occurred in both sexes and was identified as a relevant cause of death or co-morbidity particularly in males. Epithelial hyalinosis at extrapulmonary sites was noted at higher frequency in females. This study contributes important data on the spontaneous age-related pathology of the 129S6/SvEvTac mouse substrain and may represent a valuable reference for the evaluation of the phenotype in GEM obtained with this 129 substrain.

Keywords: 129 mouse, aging, blepharoconjuctivitis, Harderian gland, hyalinosis

Corresponding author: Enrico Radaelli

VIB11 Center for the Biology of Disease

KU Leuven Center for Human Genetics

O&N4 Herestraat 49 box 602

B-3000 Leuven (Belgium)

Phone: +32 16 379805

Fax: +32 16 330827

E-mail: Enrico.Radaelli@cme.vib-kuleuven.be

Introduction

Each inbred laboratory mouse strain exhibits a unique spectrum of naturally occurring lesions that develop progressively with age. Crosses of different strains usually result in variations of the original strain-specific phenotype which include vanishing, attenuation or exacerbation of expected lesions or even development of completely new conditions.[18,68] In this context, an accurate definition of strain-specific pathology in those inbred mice that are most frequently used in biomedical research [especially for the generation of genetically engineered mice (GEM)] is crucial to understand whether a phenotype results from the experimental intervention or rather reflects a naturally occurring entity.[3,51,59] In addition, longitudinal survival studies determining the aging phenotype of inbred strains are particularly important as they provide a useful reference that enables the selection of the most appropriate genetic background for specific experiments and facilitates the interpretation of clinicopathological changes developed in long-term studies.[3,42,68]

Thorough and comprehensive pathological analysis of inbred strains is important not only for interpreting lesions in the setting of hypothesis-driven research but also for identifying via large-scale forward genetic screens novel phenotype-genotype correlations that can be biologically relevant to model specific aspects of human diseases.[41] This concept holds particularly true for the analysis of aging populations where inbred mice provide a unique experimental tool because of their genetic homogeneity, short life span and the large availability of advanced technologies and comprehensive databases for studying mouse genome and phenome.[59] In this context, there are already several examples where the identification of genetic traits underlying specific age-related disorders in inbred mice have been successfully translated into

clinic proving that similar conditions in humans and mice share common pathomolecular landscapes.[41,49,59,71]

Targeted mutagenesis in mice still represents one of the most powerful tools to investigate the genetic basis of diseases. This strategy has made extensive use of the 129 mouse strain as reference source of embryonic stem (ES) cells.[3,50,51,68] Although several mouse lines are grouped under the 129 umbrella, there is a high degree of genetic variability among these different substrains as a result of either genetic drifting or accidental genetic contamination during outcrossing.[3,50,56,63,64,68] The conundrum associated with this heterogeneous genetic makeup prompted a thorough re-classification of the 129 mouse based on substrain identification and definition in terms of microsatellite markers.[56] However, the description of specific phenotypic traits associated with each of these substrains is far from being completed. In this context, studies that systematically address the aging phenotype (including the full characterization of the pathology of aging) are restricted to few investigations conducted on 129S4/SvJae mice.[3,20,68] From these studies, eosinophilic crystalline pneumonia and nephropathy clearly emerged as common non-neoplastic disorders and important cause of death/contributing cause of death (COD/CCOD).[3,20,68] Pulmonary, hepatic and Harderian gland tumors were also identified as frequent neoplastic conditions and important COD/CCOD as well.[3,68]

As comprehensive observations are limited to the 129S4/SvJae mouse, it is currently unclear to what extent the genetic variability existing among the diverse 129 mouse substrains impacts on spectrum, latency, frequency and severity of age-related pathology. While a number of background disorders may be equally represented over several sublines, major phenotypic differences are expected. Further supporting this notion, distinctive causes of morbidity and/or mortality appear to be more frequently

(or exclusively) described in specific substrains of the 129 mouse while exceedingly rare (or non-existent) in the 129S4/SvJae mouse. The 129P3/J (129/J) line appears to have an increased proclivity for the development of chronic progressive blepharoconjunctivitis.[57,60] A variety of opportunistic bacteria (e.g. *Corynebacterium* spp. and *Pasteurella pneumotropica*) have been also associated with this condition although their actual pathogenetic role is still matter of controversy.[60] In a recent study, bilateral obstructive hydronephrosis resulting from cystinuria and subsequent urolithiasis has been identified as the major cause of death in the 129S2/SvPasCrl mouse. It was then demonstrated that this substrain carries a single pathogenic mutation in the *Slc3a1* gene which encodes for a subunit of the amino acid transporter present along the brush border of the proximal renal tubules. The resulting loss of function of the transporter is pathogenetically linked to the high frequency of kidney/urinary bladder stones observed in this mouse line. Interestingly enough, mutation of the ortholog gene is responsible for the same autosomal recessive disorder in humans.[26]

In this work, we report the results of a longitudinal survival study conducted on 62 129S6/SvEvTac mice (18 females and 44 males). The investigation aimed at determining several important biological features of this inbred mouse strain including major clinical manifestations, longevity (life span), spectrum of spontaneous lesions and contributing causes of morbidity and/or mortality.

Materials and Methods

Animals and husbandry

A total of 18 female and 44 male 129S6/SvEvTac mice housed in a conventional facility were considered in this study. Animals were individually identified by means of ear tags (Small Animal Ear Tag, National Band & Tag Co., USA) and were multiply housed (up to five mice) in open polycarbonate cages (Mod. 1144B, Tecniplast, Italy) on dust-free wood litter (Lignocel® 3⁄4; Rettenmaier & Sohne, Ellwangen-Holzmühle, Germany). Standard not-autoclaved rodent diet (Teklad 2018 Global 18% Protein Rodent Diet, Harlan Teklad Diets, Madison, WI) and tap water were provided *ad libitum*. Environmental conditions were controlled with a temperature of 22°C ±2 and a 55% ±10 relative humidity. A 12/12 hours light/dark cycle with the light phase from 7:00 to 19:00 was applied. Mice were included in a health monitoring program developed in accordance with the Federation of European Laboratory Animal Science Associations (FELASA) guidelines. The colony tested positive for *Pasteurella pneumotropica*, *Entamoeba* sp., *Tritrichomonas* sp., *Aspiculuris tetraptera*, *Syphacia obvelata* and *Myobia musculi* whereas it was free from the following viral and bacterial pathogens: mouse hepatitis virus, mouse parvovirus, minute virus of mice, pneumonia virus of mice, Sendai virus, Theiler's murine encephalomyelitis virus, ectromelia virus, Hantaan virus, lymphocytic choriomeningitis virus, mouse rotavirus, *Bordetella bronchiseptica*, *Citrobacter rodentium*, *Clostridium piliforme*, *Corynebacterium kutscheri*, *Leptospira* sp., *Mycoplasma* sp., *Salmonella* sp., *Streptobacillus moniliformis*, ß-hemolitic *Streptococcus*, *Streptococcus pneumoniae*. Procedures involving animals were performed in accordance with the Italian Laws (D.L.vo 116/92 and following additions), which enforced EU 86/609 Directive (Council Directive 86/609/EEC of November 24, 1986, on the approximation of laws, regulations, and administrative provisions of the member states regarding the protection of animals used for experimental and other scientific purposes).

Animal clinical monitoring

In this longitudinal survival study, mice were allowed to live indefinitely. Animals showing signs of advanced disease or terminal conditions were sacrificed with carbon dioxide (CO_2) asphyxiation and submitted for pathological examination. Complete pathological examination was also performed on the few mice that died spontaneously. Two levels of clinical examination were routinely conducted on the animals considered in this study: (i) daily visual inspection performed by animal caretakers with the purpose of identifying major behavioral and/or clinical abnormalities; (ii) thorough clinical examination performed monthly and before the sacrifice by a certified laboratory animal veterinarian which included a careful observation of mice in their home cage followed by hands-on physical inspection.

Pathological examination

Sacrificed or spontaneously dead animals were submitted to the Department of Veterinary Sciences and Public health of the University of Milan (Milan, Italy) for complete end of life (EOL) pathological assessment including necropsy with dissection and histological examination of the following organ and tissues: brain, heart, kidneys, liver, lung, pancreas, small and large intestine, stomach, spleen, skeletal muscle (*quadriceps femoris*) skin of the dorsum, skin from the inguinal region including mammary gland, a portion of the vertebral column including spinal cord, sternum, testes with epididymis (males), ovaries and uterine horns (females), trachea, esophagus, and any additional organ/tissue showing macroscopically detectable

changes. Both eyes were excised *in toto* including Harderian glands, eyelids and conjunctiva and collected for fixation in Davidson's fluid as previously described.[24] All the other samples were immersion-fixed in 10% neutral buffered formalin, routinely processed for paraffin embedding, sectioned at 5 µm and stained with Hematoxylin and Eosin for histopathological examination. Serial sections obtained from representative lesions were also immunostained as detailed in the Supplemental Table 1. In addition, Giemsa and Gram stains were also performed on selected cases. Sternum and vertebral column were decalcified in a 14% solution of Tetrasodium EDTA for 10 days before processing and paraffin embedding.

Statistical analysis

Statistical analyses were performed using Graph Pad Prism version 5.0 (GraphPad Software, San Diego, CA). Comparisons of survival between males and females was made by using Kaplan-Meier survival curve analysis. The log-rank (Mantel-Cox) test was used to assess the difference between survival curves. The incidence of non-neoplastic and neoplastic lesions between males and females was compared using the Fisher's exact test. P values < 0.05 were considered statistically significant.

Results

Longevity (life span)

Age range for the entire mouse population considered in this study was 212 to 1160 days with females ranging between 212 and 932 days and males ranging between 292

and 1160 days. Estimated median survival time was 770 days for the entire mouse population, 770 days for females alone and 778 days for males alone with no significant difference between genders (Fig. 1).

Clinical findings and EOL assessment

Daily visual monitoring proved to be an essential measure to prevent early censoring for nonfatal but readily observable lesions (such as external masses or lesions affecting eyes, skin and perineal/genital region) and to prevent loss of pathology data due to unexpected death and postmortem degeneration (autolysis).

Frequencies of the major categories of clinical signs/abnormalities as recorded during the last physical examination before euthanasia or, in a few cases, spontaneous death are reported in Table 1. Ocular lesions consistent with blepharitis/blepharoconjuctivitis and abdominal distension emerged as the most prevalent clinical findings encountered in both sex groups [33/44 (75%) for males and 12/18 (67%) for females] and in female alone (12/18, 67%), respectively. These 2 entities, as well as other categories of nonfatal lesions including external masses or abnormalities of skin and perineal/genital region, were always associated with one or more of the following clinical signs suggestive of imminent death: (i) severe locomotor impairment, (ii) hyporesponsiveness to stimuli, (iii) slow or labored respiration, (iv) poor body condition/emaciation and (v) hunched posture.

Spectrum of pathology

Neoplastic lesions. Spectrum and frequency of neoplastic lesions are summarized in Table 2.

Epithelial neoplasms of Harderian gland emerged as the predominant tumor type within the study population (30/62, 48%) being the most frequent and the second most frequent neoplastic lesion affecting males (24/44, 54%) and females (6/18, 33%), respectively. In a proportion of cases (8/30, 27%), multicentric tumor development with bilateral involvement of both glands was observed. Females showed a higher prevalence of malignant tumors (4/6, 67%) when compared to males (6/24, 25%). Adenocarcinomas were characterized by local invasion of the soft orbital tissues with occasional extension to skull/brain and metastatic dissemination to the lungs (Figs. 2-4). Multifocal findings of myoepithelial differentiation were not uncommon in both adenomas and adenocarcinomas. However, frequency of this latter observation has not been consistently recorded.

Epithelial neoplasms of the bronchiolar/alveolar compartment (Figs. 5, 6) represented the second most common tumor category encountered within the study population (29/62, 47%) being the most frequent and the second most frequent neoplastic lesion affecting females (11/18, 61%) and males (18/44, 41%), respectively. Malignant lesions accounted for about 1/3 of the total cases of primary epithelial tumors in both genders. Adenocarcinomas were usually characterized by their large size, invasive nature, evidence of intratumoral necrosis and features of clear cytoarchitectural atypia (Fig. 6). Multicentric lesions were commonly observed although the frequency of this finding has not been consistently recorded.

Hepatocellular tumors also exhibited a relatively high prevalence within the study population (18/62, 29%) with males more affected than females [15/44 (34%) for males and 3/18 (17%) for females]. In addition, malignant lesions (Fig. 7) accounted for more

than 1/3 of the total cases of hepatocellular tumors in males whereas only benign lesions were observed in females.

Uterus (together with the Harderian gland) represented the second most common site of tumor development in females with 6 out of 18 (33%) affected animals. Tumor spectrum in this organ was heterogeneous including 3 sarcomas arising from the endometrial stroma and single cases of endometrial adenocarcinoma, hemangioma and leiomyoma.

Prevalence of hematopoietic malignancies within the study population was relatively low (8/62, 13%). By the time of necropsy, all the hematopoietic tumors have reached an advanced stage of development showing multicentric growths and/or dissemination to multiple organs and tissues. A total of 5 lymphomas (4 occurring in males and 1 in females) were observed. Immunohistochemical characterization of the lymphoid neoplasm affecting the female mouse indicated the development of a histiocyte-associated B cell lymphoma. Two histiocytic sarcomas were observed in one animal per sex. The tumor noted in the male mouse was characterized by a mass at the level of the epididymis, with extensive dissemination to lungs, spleen, liver, kidneys, lymph nodes and bone marrow (Supplemental Figs. 1-3). The case observed in the female arose in the uterus with local spread to the mesovarium and was characterized by massive necrosis of the affected tissues. Immunohistochemistry for F4/80 and IBA1 confirmed the histiocytic origin of these neoplasms (Supplemental Figs. 2, 3). Lastly, a single case of mast cell sarcoma was recognized in a male subject. The tumor displayed a very aggressive nature with a large subcutaneous mass (most likely representing the primary site of development) and massive involvement of lungs, spleen, liver, kidneys, lymph nodes, bone marrow and skin. Giemsa stain of representative lesions in different organs and tissues demonstrated a prominent

granular metachromasia in the cytoplasm of neoplastic cells confirming the mast cell nature of the tumor (Supplemental Fig. 4).

Other tumor categories occurred with a very low frequency both in males and in females. Notably, 3 cases of brain ependymoma were described in males. All the reported lesions showed a clear periventricular distribution and focal continuity with the ependymal lining in at the level of the foramina of Monro/third ventricle. Microscopically, ependymomas consisted of tumor cells arranged in pseudorosettes around a prominent vascular network. All the reported ependymomas displayed features of malignancy including intratumoral necrohemorragic foci and multifocal invasion of the surrounding neuroparenchyma. Immunohistochemically, tumors appeared invariably negative for glial fibrillary acidic protein (GFAP) but exhibited diffuse vimentin positivity and wide spectrum cytokeratin (WSCK) expression in about 20% of tumor cells.

Non-neoplastic lesions. Spectrum and frequency of non-neoplastic lesions are summarized in Table 3.

Blepharitis/blepharoconjunctivitis emerged as the most prevalent non-neoplastic condition both in males (38/42, 90%) and females (15/16, 94%). Most of the affected mice (31 males and 15 females) exhibited bilateral eye involvement. Histologically, different degrees of lesion severity were recognized. Mildest cases showed epidermal acanthosis and hyperkeratosis of the eyelids associated with crusting of the mucocutaneous junction and minimal infiltrates of inflammatory cells in the subjacent dermis/lamina propria. In more severe cases, eyelids and conjunctival mucosa were involved by suppurative inflammation often accompanied by mucocutaneous erosion/ulceration (Figs. 8, 9). A statistically significant association was not identified

for the concurrent development of blepharoconjuctivitis and Harderian gland tumor. In a large proportion of cases (19 males and 11 females), Gram staining disclosed the presence of positive bacteria in the form of short and occasionally curved rods. Gram-positive bacteria were frequently noted in association with the keratin debris accumulating along the eyelid rim (Fig. 9). As detailed in the Supplemental results and Supplemental Table 2, follow-up clinicopathological and microbiological investigations were conducted to define nature and role of Gram-positive rods often described in association with blepharitis/blepharoconjunctivitis.

Accumulation of eosinophilic crystals in the lumen of bronchi/bronchioles and alveoli represented the second most common non-neoplastic lesion encountered in both males (30/44, 68%) and females (13/18, 72%). Eosinophilic crystalline pneumonia (ECP), formerly known as acidophilic macrophage pneumonia, was also identified as highly frequent non-neoplastic lesion affecting up to 60% of mice in both sex groups. Pulmonary accumulation of eosinophilic crystals and ECP were often accompanied by hyalinosis of bronchial/bronchiolar epithelium (Figs. 6, 10). Other organs and tissues exhibiting epithelial hyalinosis were, in order of frequency, glandular mucosa of the stomach [recorded in 4/44 (9%) males and 4/18 (22%) females], gall bladder/bile ducts [recorded in 3/44 (7%) males and 3/18 (17%) females], transitional epithelium of renal pelvis [only detected in 2 out of 18 females] and pancreatic ducts [only detected in 1 out of 44 males] (Supplemental Figs. 5-7). Based on these findings, the frequency of epithelial hyalinosis affecting extrapulmonary sites resulted significantly higher in 129S6/SvEvTac females. Lastly, regardless of the sex of affected animals or type of tissue involved, hyalinosis was consistently accompanied by different degrees of epithelial hyperplasia and inflammatory cell infiltrates with a prominent eosinophilic component (Supplemental Figs. 5-7).

Non-neoplastic lesions affecting the cardiovascular system were also highly represented in the aging mouse cohort considered in this study. Progressive cardiomyopathy was observed in more than 50% (33/62, 53%) of the examined mice with males slightly more affected than females. Early myocardial lesions consisted of individual cardiomyocyte degeneration and necrosis. In more severe and chronic cases, cardiomyocyte degeneration and necrosis was accompanied by interstitial fibrosis and infiltration of mononuclear inflammatory cells (Supplemental Fig. 8). Polyarteritis also exhibited a relatively high frequency within the male population (15/44, 34%) whereas females mice were completely unaffected. The condition was characterized by a combination of necrotizing and/or proliferative inflammatory changes segmentally affecting the tunica media of small to mid-sized arteries in several tissues including heart, pancreas, spleen, kidneys, gastrointestinal and reproductive tracts (Fig. 11).

The female genital tract represented another major site of non-neoplastic lesions development. The uterus of more than 70% (12/17) of the examined females presented degenerative and proliferative changes compatible with cystic endometrial hyperplasia (Fig. 12). Angiectasis and thrombosis of myometrial/endometrial blood vessels and suppurative metritis/pyometra also emerged as highly frequent uterine lesions being observed in about half of the females (Fig. 12). In addition, peritonitis was identified as a lethal complication of suppurative metritis/pyometra in 4 females.

Fibro-osseous lesion was another relatively frequent non-neoplastic change that was almost exclusively observed in females (7 out of 17 affected females with only 1 case in over 44 males). Lesions, mainly affecting epiphyseal/metaphyseal extremities of long bones, were characterized by irregular proliferations of dense fibrovascular tissue with extensive effacement of bone marrow and osteoclastic trabecular bone resorption.

More advanced cases displayed a clear osteosclerotic progression of the initial fibroproliferative changes with original bone marrow lacunae almost completely obscured by thick bony trabeculae (Supplemental Fig. 8).

Other minor changes that were reported with a significantly higher frequency in the female group included foci of extramedullary hematopoiesis in the liver, increased extramedullary hematopoiesis in the splenic red pulp, lymphoid depletion affecting the splenic white pulp, reactive myeloid hyperplasia of the bone marrow and plasmacytosis in the lymph nodes.

Minimal to mild infiltrates/foci of inflammatory cells were detected in a wide range of tissues being the most frequent non-neoplastic changes observed in the liver of males (19/44, 43%) and kidneys of both genders [22/43 (51%) for males and 13/18 (72%) for females].

Ovaries and lower urogenital tract including urinary bladder and most of the male accessory sex glands were not consistently analyzed histologically or sometimes comprised in the evaluation only when affected by grossly detectable changes. In this context, the real prevalence of the different lesions observed in these organs and tissues cannot be inferred with accuracy.

COD/CCOD

Major contributory causes of morbidity and death are summarized in Table 4. A single tumor was identified as the major cause of death in 11 males and 4 females. Hematopoietic tumors were the most common neoplastic conditions noted as single major COD in males, followed by hepatocellular and gastrointestinal tumors. One male succumbed to an anaplastic metastatic tumour apparently arising from a testicle.

Immunohistochemistry failed to support a definitive classification of this neoplasm. Tumours identified as single major COD in females included an adenocarcinoma of the Harderian gland characterised by invasion of the skull and brain and metastatic dissemination to the lungs, a hemangiosarcoma arising in the skin of the tail with pulmonary and hepatic metastases, an adenoma of the pituitary pars distalis and a lymphoma with multisystemic dissemination.

Polyarteritis represented a major CCOD in 6 males. Eosinophilic crystalline pneumonia was identified as single COD in 4 males and 2 females. Urologic syndrome was found as COD in 2 males and represented a significant co-morbidity in another male. Peritonitis resulting from suppuration and necrosis of seminal vesicles was considered as primary COD in an additional male. Suppurative metritis/pyometra, in most cases with associated peritonitis, was confirmed as cause of death in 4 females. Two males and 2 females died because of sepsis (Supplemental Fig. 9). Megaesophagus was identified as primary COD in 1 male.

In several instances multiple disease conditions were identified as concurrent CCOD. These included multiple non-neoplastic lesions (in 9 males and 1 female) or concurrent neoplastic and non-neoplastic conditions (in 7 males and 3 females). In this context polyarteritis, cardiomyopathy and preputial gland suppurative adenitis/abscessation were noted as relevant co-morbidities in males (Supplemental Fig. 10). Megaesophagus was noted as significant co-morbidity in 4 male and 1 female. Eosinophilic crystalline pneumonia (ECP) was identified as co-morbidity along with pulmonary adenocarcinoma and other non-neoplastic conditions in 4 males. ECP was also noted as contributory cause of death in 2 females, in both cases in association with uterine angiectasis/thrombosis. Presence of a uterine tumour (hemangioma) or development of sepsis were also considered as significant co-morbidities in these 2

mice. Ependymomas noted in the brain of 3 males were considered as contributory causes of death, but in all case as co-morbidities associated with concurrent tumors or non-neoplastic lesions.

In 2 males a contributory cause of death could not be identified on the basis of the available pathology data.

Discussion

In this work we report a longitudinal aging study conducted on 129S6/SvEvTac mice providing a comprehensive overview of the full spectrum of spontaneous age-related disorders occurring in 44 males and 18 females. While our study was mainly focused on defining at pathological level nature and frequency of age-related lesions, other relevant experimental features including major contributory causes of morbidity and death, clinical manifestations and longevity (life span) have been also investigated in detail.

Epithelial tumors affecting Harderian gland and bronchioloalveolar compartment emerged as the most common neoplastic lesions encountered in both genders. A striking prevalence of the same tumor categories has been also previously described by Ward and colleagues in a cohort of aging 129S4/SvJae mice.[68] Mouse Harderian gland and bronchioloalveolar compartment are preferential targets of oncogenic *K-ras* and *H-ras* activity. The correlation between activating *K-ras* mutations and concurrent development of epithelial tumors from both locations has been widely documented in carcinogenicity studies.[21,54,55] A role for *H-ras* oncogene during pulmonary and/or Harderian gland tumorigenesis has been also demonstrated in spontaneously occurring cases as well as in transgenic mice overexpressing the human c-Ha-ras

oncogene.[5,16,36] Interestingly, proclivity for the development of spontaneous pulmonary tumors in the 129 mouse appears to be directly linked with a specific *pulmonary adenoma susceptibility 1* (*Pas1*) haplotype which leads to constitutive overexpression of *K-ras* in the lung.[7] In this context, it can be hypothesized that an identical or similar molecular mechanism might be also responsible for the high incidence of Harderian gland tumors in the same mouse strain.

Similarly to what has been reported for the 129S4/SvJae subline, hematopoietic tumors rarely occurred in 129S6/SvEvTac mice.[68] Despite their low frequency, hematopoietic malignancies represented an important COD because of their disseminated nature with extensive involvement of multiple organ and tissues. Notably, we identified an unusual but distinctive case of disseminated mast cell sarcoma. A large multinodular mass in the dermis/subcutis was tentatively identified as primary lesion. However, because of the extensive involvement of most of the examined organs/tissues, the actual site of tumor origin could not be established with accuracy and a possible multicentric evolution of the lesion was also considered. The mast cell disorder reported in the 129S6/SvEvTac mouse recapitulates some of the most representative pathobiological features of systemic mastocytosis in humans including concurrent cutaneous involvement and multicentric growth/systemic dissemination to visceral organs and bone marrow.[31] Despite a series of proliferative mast cell disorders have been documented in chemically-induced or genetically engineered mouse models,[15,31,38,62] naturally occurring lesions remains exceedingly rare.[13] Description of spontaneous mast cell tumors is limited to sporadic cases occurred in diverse mouse strains including CD-1, BALB/c, B6C3F1, CFLP, C57BL/6 and four-way cross mice.[6,12,13,25,27] Similarly to what has been observed in our study, the great majority of these spontaneous lesions exhibited an aggressive behavior with systemic

dissemination/multicentric growth at the level of skin, bone marrow and visceral organs.

Ependymoma, another unique neoplasm here diagnosed in 3 males, is considered an exceedingly rare spontaneous lesion in the mouse.[1,23] A recent retrospective database analysis identified 3 cases of ependymoma on a total of over 100.000 mice surveyed.[1] In view of these data, the frequency of ependymomas observed in our cohort appears unexpectedly high. In this context, the analysis of a larger number of aging animals may clarify whether these tumors simply represent an incidental finding or a real predisposition for ependymal neoplasms exists in the 129S6/SvEvTac substrain. Microscopically, all the 3 brain tumors here reported showed the typical diagnostic features of a rodent ependymoma including periventricular distribution, prominent vascular network (microvascular proliferation), perivascular pseudorosettes without evidences of luminal rosettes. All the 3 ependymomas were also designed as malignant based on the evidence of intratumoral necrosis and/or invasion of the surrounding neuroparenchyma.[1,23] Immunohistochemical examination confirmed lack of GFAP expression and diffuse vimentin positivity, features which have been considered characteristic for rodent ependymoma.[1] In addition, individual tumor cells displayed unequivocal cytoplasmic WSCK immunoreactivity. The cytokeratin expression profile in murine ependymoma is currently unexplored. However, positive cytokeratin immunostaining is a well-documented aspect in ependymal tumors arising from humans, cats and dogs.[32,52,65,70]

In our study, an accurate and reliable comparison of tumor frequencies between genders has been often made difficult by the significantly smaller sample size of the female cohort. Nevertheless, major sex-related variations could be identified for some of the most frequent neoplastic categories.

Despite an overall higher prevalence of Harderian gland tumors in males, malignant lesions were more commonly reported in females where they showed a particularly aggressive behavior with local invasion of the skull/brain and metastatic spread to the lungs. Interestingly, the same higher male prevalence of Harderian gland tumor was described also in 129S4/SvJae mice but malignant lesions occurred only sporadically in this substrain without a clear gender bias.[3,68]

Regarding the occurrence of primary pulmonary tumors, 129S6/SvEvTac females were considerably more affected than males. This female predisposition is in net contrast with the data resulting from the analysis of aging 129S4/SvJae mice where exactly the opposite situation has emerged for pulmonary tumors.[3,68]

Not surprisingly, an obvious gender predisposition was also identified in hepatocellular tumors with 129S6/SvEvTac males much more affected than females. This evidence appears even more substantial considering that malignant lesions, in the form of hepatocellular carcinoma, occurred only in males where they represented an important neoplastic COD/CCOD. In the mouse, like in other species including humans, hepatocellular tumors (especially carcinomas) represent a male-predominant condition.[45] Increased male susceptibility to spontaneous hepatocellular tumors is obvious in most inbred mouse strains including the 129S4/SvJae subline.[3,68] Male predisposition is seen not only in the context of spontaneous hepatic tumorigenesis but also in diverse experimental settings including the induction of liver tumors by a wide variety of carcinogens or infectious agents.[4,44] Endocrine ablation studies have demonstrated that the difference in gender susceptibility results from the opposing effects of male and female sex hormones, with testosterone enhancing and ovarian hormones and prolactin inhibiting hepatocellular tumor development.[4,19]

Blepharitis/blepharoconjunctivitis represented by far the most prevalent non-neoplastic age-related disorder affecting both male and female 129S6/SvEvTac mice. Naturally occurring episodes of ulcerative blepharoconjunctivitis have been only occasionally reported in laboratory mice.[57] Some inbred lines of mice including BALB/c, C57BL/6 and 129P3/J appear to be more commonly affected than others.[40] In these predisposed strains, ulcerative blepharoconjuctivitis often manifests as a common age-related disorder. A variety of opportunistic bacteria (e.g. *Corynebacterium* spp., *Staphylococcus aureus*, *Staphylococcus xylosus*, *Pasteurella pneumotropica*) have been also correlated with the episodes of blepharoconjunctivitis although their effective pathogenetic role is still matter of controversy.[60] Corynebacteria in particular have been identified in outbreaks involving aging mice.[40,57,60] In one study investigating the occurrence of spontaneous blepharoconjuctivitis in a colony of 129P3/J mice, Sundberg and collaborators reported that the frequency of affected individuals from both sexes increased progressively involving approximately the 50% of animals aged 30 or more weeks. An uncharacterized corynebacterial species was consistently isolated from the affected eyes.[60] An epizootic of ulcerative conjunctivitis and keratitis associated with an unidentifiable *Corynebacterium* spp. was also reported in a colony of male C57BL/6 mice. Ocular lesions were first detected at 18 months of age and their incidence and severity increased dramatically to involve over the 90% of 21 to 30 month-old mice.[30]

Also in our study, diverse corynebacterial species have been commonly isolated form ocular lesions. However, overall data emerging from follow-up clinicopathological and microbiological investigations do not support an unequivocal causative association between isolated bacteria and blepharitis/blepharoconjuctivitis. All the identified corynebacterial species have been previously described as common inhabitants of

mouse skin without specific pathogenic capabilities in immunocompetent hirsute mice.[10,11,14,37,46,48] In this context, the reason of their frequent recovery from the conjunctival surface and the role played in the development and progression of ocular lesions are currently undetermined. We hypothesize that age-related structural and/or functional changes of eyelids and lacrimal system may have contributed to impair the integrity of mucocutaneous epithelial barrier thus promoting chronic inflammation of and facilitating the colonization of the palpebral conjunctiva by commensal bacteria normally residing on the skin.[30,40,42] Further supporting this view, anterior migration of the palpebral mucocutaneous junction represents a well-documented age-related condition in mice where it is mainly associated with eyelid laxity and meibomian gland atrophy and dysfunction.[39,58] Atrophy and dysfunction of the lacrimal glands are also very commonly reported in aging mice and may result in decreased tear production and secondary conjunctivitis.[42]

ECP, formerly known as Acidophilic Macrophage Pneumonia (AMP), has been described as a major cause of disease and death in C57BL/6 mutant mice deficient in SHP-1 protein-tyrosine phosphatase (“motheaten” and “viable motheaten”).[53,67] ECP has been reported with variable incidence in different mouse strains,[35] and has also been characterized as a frequent pulmonary lesion and significant cause of morbidity and mortality in 129S4/SvJae mice.[20,68,69] Epithelial cytoplasmic hyaline change, commonly referred to as “hyalinosis”, affecting the nasal respiratory and olfactory epithelium, the tracheal and bronchial epithelium (with or without concurrent ECP), the glandular stomach, bile duct and pancreatic duct epithelium, has been reported in mice of the 129S4/SvJae substrain and in the B6;129 mouse line.[68,69] Accumulation of proteins of the Ym family (mammalian chitinase-like lectins) has been identified as the mechanism underlying the accumulation of intrahistiocytic and extracellular

558 eosinophilic crystals in ECP and epithelial hyalinosis of the upper respiratory
559 epithelium, glandular stomach, biliary and pancreatic ducts.[17,69]
560 In our study, pulmonary accumulation of eosinophilic crystals and ECP were frequently
561 observed and often combined lesions with overall comparable incidence in male and
562 females. ECP was also identified as major COD/CCOD and significant co-morbidity in
563 both sex groups. Similarly to what has been reported for the 129S4/SvJae subline,
564 epithelial hyalinosis in extrapulmonary sites was more prevalent in 129S6/SvEvTac
565 females (Ward et al. 2001). Hyaline changes were recorded in the epithelium of
566 glandular stomach and bile ducts/gall bladder in both sexes. Hyalinosis of the
567 pancreatic duct epithelium was noted in a single male. Interestingly, hyalinosis of the
568 transitional epithelium of the renal pelvis was noted in 2 females in association with
569 inflammation or hydronephrosis. Hyalinosis and eosinophilic crystal formation related
570 to accumulation of Ym proteins has been reported in a case of polypoid adenoma of
571 the transitional epithelium of the renal pelvis in a *PML/RAR*α knock in mouse with acute
572 myeloid leukemia.[28] In addition, in a study dissecting the molecular pathogenesis of
573 ureteritis leading to early onset hydronephrosis in the F2 progeny of C57BL/6 and
574 DBA/2 mice, eosinophilic crystals formation with upregulation and accumulation of
575 Chi3l3/Ym1 protein has been shown to occur in association with hyperplasia of the
576 transitional epithelium.[22] Immunohistochemistry confirmed accumulation of
577 Chi3l3/Ym1 within macrophages and in extracellular crystals within bronchial/alveolar
578 lumens in ECP, and in epithelial cells affected by hyalinosis in the above mentioned
579 tissues.
580 Major non-neoplastic conditions with an obvious gender predisposition included FOL
581 and polyarteritis.

582 While FOL represented a relatively frequent disorder in 129S6/SvEvTac females (7 out
583 of 17 affected females), only one case was confirmed in males. FOL has been already
584 described as age-related disorder almost exclusively affecting female mice.[2,47,66] The
585 pathogenesis of this condition appears to be driven by age-related hormonal
586 imbalances of the female reproductive system. Some mouse lines (including the
587 129S4/SvJae substrain) are reportedly more susceptible than others indicating that
588 specific genetic backgrounds may further enhance the hormonal impact.[2,66,68]
589 Experimental evidences supporting these mechanisms were provided by the
590 observation that synthetic compounds with hormonal activity like diethylstilbestrol and
591 misoprostol also induce a high incidence of FOL in female mice while males are only
592 marginally affected.[29] In addition, a causative association between age-related lesions
593 of female reproductive tract (e.g. ovarian atrophy, ovarian cysts and cystic endometrial
594 hyperplasia) and development FOL has been also proposed.[2,9,66] A similar correlation
595 could not be confirmed in our study since all the examined females were ultimately
596 affected by multiple and often concurrent uterine and ovarian lesions.
597 A distinctive proclivity for the development of polyarteritis was observed in
598 129S6/SvEvTac males while the same disorder was never reported in females. For
599 their severity (especially when affecting vital organs) and multisystemic nature,
600 vascular lesions were often considered significant CCOD. An obvious male
601 predisposition for arteritis has been also previously documented in the 129S4/SvJae
602 substrain while an opposite trend was noted in B6;129 mice.[3,18,68] Immune-mediated
603 mechanisms have been proposed to play a pivotal role in the pathogenesis
604 spontaneous polyarteritis in aging mice.[40,42] In this context, lifelong expression of
605 proteins encoded by endogenous retroviruses/retroelements has been considered as
606 the event potentially responsible for most of the immune-mediated disorders in aging

mice including glomerulonephritis and polyarteritis.[33,40,61] On the other hand, several lines of evidence indicate that hypertension may also have a primary role in the development of murine polyarteritis.[34] Interestingly, in a study assessing different cardiovascular traits among 11 commonly used inbred mouse strains, male 129S1/SvImJ mice exhibited the highest systolic blood pressure values.[8] Assuming that the same male-predominant high blood pressure phenotype is equally represented among different 129 sublines, the development of a hypertensive state in aging 129S6/SvEvTac males can be potentially correlated to the pathogenesis of polyarteritis.

As frequently observed in other mouse strains including 129S4/SvJae and B6;129 mice,[18,68] chronic progressive cardiomyopathy emerged as classical age-related disorder also in 129S6/SvEvTac mice with overall comparable incidence in male and females. Different degrees of myocardial involvement were recognized with more severe lesions ultimately considered as a relevant co-morbidity especially among male mice.

In both sex groups of 129S6/SvEvTac mice, suppurative inflammation of the urogenital tract and accessory sex glands (with or without evidence of bacterial infection) represented an important lesion category not only in terms of frequency but also with a relevant impact as COD/CCOD or co-morbidity. The entity in females was mainly characterized by pyometra/suppurative metritis often evolving to peritonitis as lethal complication. Abscessation of the preputial gland was reported as the most common manifestation in males, whereas necrosuppurative inflammation of the seminal vesicles or prostate occurred at lower frequency. Cellulits/fasciitis of the inguino-pubic region and peritonitis represented clinically relevant and perhaps lethal complications of lesions affecting preputial glands and seminal vesicles, respectively. A variety of

opportunistic bacteria including *Pasteurella pneumotropica*, *Klebsiella oxytoca* and staphylococci are normally responsible for the development suppurative lesions affecting the urogenital tract and accessory sex glands.[40,43] Unfortunately, the cases reported in our study were not investigated microbiologically and an etiology could not be defined.

In conclusion, this study demonstrates that major neoplastic and non-neoplastic conditions affecting aging 129S6/SvEvTac mice have been previously reported also for other 129 substrains with no substantial differences in terms of distribution and frequency.[3,60,68] In addition, our data confirm that the 129 background is actually "resistant" to a series of classical age-related disorders (including hematopoietic and mammary tumors, amyloidosis, rectal prolapse and dermatitis) commonly encountered in other strains of mice including backcrossed 129 lines.[3,18,40,42,68] Overall, these findings reinforce the idea that, while a high degree of genetic variability exists within the 129 strain, dominant age-related phenotypic traits are equally represented over several sublines.

We believe that this work marks an important contribution as it defines the background pathology of a 129 substrain that has been widely used for the generation of targeted mutant mouse lines. In this context, the information contained in this paper can represent a solid reference for the interpretation of spontaneous aging lesions in inbred 129S6/SvEvTac mice and incompletely backcrossed strains where targeted mutation has been originally generated in 129S6/SvEvTac mice ES cells.

Acknowledgements

We are grateful for the excellent technical assistance of Maurizio Barzani, Marco Brevi and Marco Losa.

Declaration of Conflicting Interests

The author(s) declared no potential conflicts of interest with respect to the research, authorship, and/or publication of this article.

Funding

The author(s) received no financial support for the research, authorship, and/or publication of this article.

References

1 Adams ET, Auerbach S, Blackshear PE, et al. Proceedings of the 2010 National Toxicology Program Satellite Symposium. *Toxicol Pathol*. 2011;**39:** 240-266

2 Albassam MA, Wojcinski ZW, Barsoum NJ, Smith GS: Spontaneous fibro-osseous proliferative lesions in the sternums and femurs of B6C3F1 mice. Vet Pathol **28:** 381-388, 1991

3 Brayton CF, Treuting PM, Ward JM: Pathobiology of aging mice and GEM: background strains and experimental design. Vet Pathol **49:** 85-105, 2012

4 Bugni JM, Poole TM, Drinkwater NR: The little mutation suppresses DEN-induced hepatocarcinogenesis in mice and abrogates genetic and hormonal modulation of susceptibility. Carcinogenesis **22:** 1853-1862, 2001

5 Candrian U, You M, Goodrow T, Maronpot RR, Reynolds SH, Anderson MW: Activation of protooncogenes in spontaneously occurring non-liver tumors from C57BL/6 x C3H F1 mice. Cancer Res **51:** 1148-1153, 1991

6 Chrisp CE, Turke P, Luciano A, Swalwell S, Peterson J, Miller RA: Lifespan and lesions in genetically heterogeneous (four-way cross) mice: a new model for aging research. Vet Pathol **33:** 735-743, 1996

7 Dassano A, Colombo F, Trincucci G, Frullanti E, Galvan A, Pettinicchio A, De Cecco L, Borrego A, Martinez Ibanez OC, Dragani TA, Manenti G: Mouse pulmonary adenoma susceptibility 1 locus is an expression QTL modulating Kras-4A. PLoS Genet **10:** e1004307, 2014

8 Deschepper CF, Olson JL, Otis M, Gallo-Payet N: Characterization of blood pressure and morphological traits in cardiovascular-related organs in 13 different inbred mouse strains. J Appl Physiol (1985) **97:** 369-376, 2004

9 Dodd DC, Port CD: Hyperostosis of the marrow cavity caused by misoprostol in CD-1 strain mice. Vet Pathol **24:** 545-548, 1987

10 Dole VS, Henderson KS, Fister RD, Pietrowski MT, Maldonado G, Clifford CB: Pathogenicity and genetic variation of 3 strains of Corynebacterium bovis in immunodeficient mice. J Am Assoc Lab Anim Sci **52:** 458-466, 2013

11 Duga S, Gobbi A, Asselta R, Crippa L, Tenchini ML, Simonic T, Scanziani E: Analysis of the 16S rRNA gene sequence of the coryneform bacterium associated with hyperkeratotic dermatitis of athymic nude mice and development of a PCR-based detection assay. Mol Cell Probes **12:** 191-199, 1998

12 Frith CH, Sprowls RW, Breeden CR: Mast cell neoplasia in mice. Lab Anim Sci **26:** 478-481, 1976

13 Frith CH, Ward JM, Chandra M: The morphology, immunohistochemistry, and incidence of hematopoietic neoplasms in mice and rats. Toxicol Pathol **21:** 206-218, 1993

14 Gobbi A, Crippa L, Scanziani E: Corynebacterium bovis infection in immunocompetent hirsute mice. Lab Anim Sci **49:** 209-211, 1999

15 Godfraind C, Louahed J, Faulkner H, Vink A, Warnier G, Grencis R, Renauld JC: Intraepithelial infiltration by mast cells with both connective tissue-type and mucosal-type characteristics in gut, trachea, and kidneys of IL-9 transgenic mice. J Immunol **160:** 3989-3996, 1998

16 Goodrow TL, Nichols WW, Storer RD, Anderson MW, Maronpot RR: Activation of H-ras is prevalent in 1,3-butadiene-induced and spontaneously occurring murine Harderian gland tumors. Carcinogenesis **15:** 2665-2667, 1994

718 17 Guo L, Johnson RS, Schuh JC: Biochemical characterization of endogenously
719 formed eosinophilic crystals in the lungs of mice. J Biol Chem **275:** 8032-8037,
720 2000
721 18 Haines DC, Chattopadhyay S, Ward JM: Pathology of aging B6;129 mice. Toxicol
722 Pathol **29:** 653-661, 2001
723 19 Hartwell HJ, Petrosky KY, Fox JG, Horseman ND, Rogers AB: Prolactin prevents
724 hepatocellular carcinoma by restricting innate immune activation of c-Myc in
725 mice. Proc Natl Acad Sci U S A **111:** 11455-11460, 2014
726 20 Hoenerhoff MJ, Starost MF, Ward JM: Eosinophilic crystalline pneumonia as a
727 major cause of death in 129S4/SvJae mice. Vet Pathol **43:** 682-688, 2006
728 21 Hong HH, Houle CD, Ton TV, Sills RC: K-ras mutations in lung tumors and tumors
729 from other organs are consistent with a common mechanism of ethylene oxide
730 tumorigenesis in the B6C3F1 mouse. Toxicol Pathol **35:** 81-85, 2007
731 22 Ichii O, Otsuka S, Namiki Y, Hashimoto Y, Kon Y: Molecular pathology of murine
732 ureteritis causing obstructive uropathy with hydronephrosis. PLoS One **6:**
733 e27783, 2011
734 23 Kaufmann W, Bolon B, Bradley A, Butt M, Czasch S, Garman RH, George C,
735 Groters S, Krinke G, Little P, McKay J, Narama I, Rao D, Shibutani M, Sills R:
736 Proliferative and nonproliferative lesions of the rat and mouse central and
737 peripheral nervous systems. Toxicol Pathol **40:** 87S-157S, 2012
738 24 Latendresse JR, Warbrittion AR, Jonassen H, Creasy DM: Fixation of testes and
739 eyes using a modified Davidson's fluid: comparison with Bouin's fluid and
740 conventional Davidson's fluid. Toxicol Pathol **30:** 524-533, 2002
741 25 Lewis DJ, Offer JM: Malignant mastocytoma in mice. J Comp Pathol **94:** 615-620,
742 1984

743 26 Livrozet M, Vandermeersch S, Mesnard L, Thioulouse E, Jaubert J, Boffa JJ,
744 Haymann JP, Baud L, Bazin D, Daudon M, Letavernier E: An animal model of
745 type A cystinuria due to spontaneous mutation in 129S2/SvPasCrl mice. PLoS
746 One **9:** e102700, 2014
747 27 Majeed SK: Mast cell tumours in CD-1 mice. Arzneimittelforschung **41:** 175-178,
748 1991
749 28 Marchesi F, Minucci S, Pelicci PG, Gobbi A, Scanziani E: Immunohistochemical
750 detection of Ym1/Ym2 chitinase-like lectins associated with hyalinosis and
751 polypoid adenomas of the transitional epithelium in a mouse with acute myeloid
752 leukemia. Vet Pathol **43:** 773-776, 2006
753 29 McAnulty PA, Skydsgaard M: Diethylstilbestrol (DES): carcinogenic potential in
754 Xpa-/-, Xpa-/- / p53+/-, and wild-type mice during 9 months' dietary exposure.
755 Toxicol Pathol **33:** 609-620, 2005
756 30 McWilliams TS, Waggie KS, Luzarraga MB, French AW, Adams RJ:
757 Corynebacterium species-associated keratoconjunctivitis in aged male
758 C57BL/6J mice. Lab Anim Sci **43:** 509-512, 1993
759 31 Merz H, Kaehler C, Hoefig KP, Branke B, Uckert W, Nadrowitz R, Cerny-Reiterer
760 S, Herrmann H, Feller AC, Valent P: Interleukin-9 (IL-9) and NPM-ALK each
761 generate mast cell hyperplasia as single 'hit' and cooperate in producing a
762 mastocytosis-like disease in mice. Oncotarget **1:** 104-119, 2010
763 32 Michimae Y, Morita T, Sunagawa Y, Sawada M, Okamoto Y, Shimada A:
764 Anaplastic ependymoma in the cervical spinal cord of a maltese dog. J Vet Med
765 Sci **66:** 1155-1158, 2004
766 33 Miyazawa M, Tabata N, Fujisawa R, Hashimoto K, Shiwaku H, Takei YA: Roles of
767 endogenous retroviruses and platelets in the development of vascular injury in

spontaneous mouse models of autoimmune diseases. Int J Cardiol **75 Suppl 1:** S65-73; discussion S75-66, 2000

34 Mullink JW, Haneveld GT: Polyarteritis in mice due to spontaneous hypertension. J Comp Pathol **89:** 99-106, 1979

35 Murray AB, Luz A: Acidophilic macrophage pneumonia in laboratory mice. Vet Pathol **27:** 274-281, 1990

36 Nambiar PR, Turnquist SE, Morton D: Spontaneous tumor incidence in rasH2 mice: review of internal data and published literature. Toxicol Pathol **40:** 614-623, 2012

37 Nieto E, Vindel A, Valero-Guillen PL, Saez-Nieto JA, Soriano F: Biochemical, antimicrobial susceptibility and genotyping studies on Corynebacterium urealyticum isolates from diverse sources. J Med Microbiol **49:** 759-763, 2000

38 Ohmori T, Mori H, Rivenson A: A study of tobacco carcinogenesis XX: mastocytoma induction in mice by cigarette smoke particulates ("cigarette tar"). Am J Pathol **102:** 381-387, 1981

39 Parfitt GJ, Xie Y, Geyfman M, Brown DJ, Jester JV: Absence of ductal hyper-keratinization in mouse age-related meibomian gland dysfunction (ARMGD). Aging (Albany NY) **5:** 825-834, 2013

40 Percy DH, Barthold SW: Mouse. *In*: Pathology of laboratory rodents and rabbits, eds. Percy DH, Barthold SW, 3rd ed., pp. 3–124. Blackwell Pub., Ames, Iowa, 2007

41 Peters LL, Robledo RF, Bult CJ, Churchill GA, Paigen BJ, Svenson KL: The mouse as a model for human biology: a resource guide for complex trait analysis. Nat Rev Genet **8:** 58-69, 2007

42 Pettan-Brewer C, Treuting PM: Practical pathology of aging mice. Pathobiol Aging Age Relat Dis **1**, 2011

43 Radaelli E, Manarolla G, Pisoni G, Balloi A, Aresu L, Sparaciari P, Maggi A, Caniatti M, Scanziani E: Suppurative adenitis of preputial glands associated with Corynebacterium mastitidis infection in mice. J Am Assoc Lab Anim Sci **49:** 69-74, 2010

44 Rogers AB, Boutin SR, Whary MT, Sundina N, Ge Z, Cormier K, Fox JG: Progression of chronic hepatitis and preneoplasia in Helicobacter hepaticus-infected A/JCr mice. Toxicol Pathol **32:** 668-677, 2004

45 Rogers AB, Theve EJ, Feng Y, Fry RC, Taghizadeh K, Clapp KM, Boussahmain C, Cormier KS, Fox JG: Hepatocellular carcinoma associated with liver-gender disruption in male mice. Cancer Res **67:** 11536-11546, 2007

46 Russo M, Invernizzi A, Gobbi A, Radaelli E: Diffuse scaling dermatitis in an athymic nude mouse. Vet Pathol **50:** 722-726, 2013

47 Sass B, Montali RJ: Spontaneous fibro-osseous lesions in aging female mice. Lab Anim Sci **30:** 907-909, 1980

48 Scanziani E, Gobbi A, Crippa L, Giusti AM, Pesenti E, Cavalletti E, Luini M: Hyperkeratosis-associated coryneform infection in severe combined immunodeficient mice. Lab Anim **32:** 330-336, 1998

49 Schofield PN, Sundberg JP, Hoehndorf R, Gkoutos GV: New approaches to the representation and analysis of phenotype knowledge in human diseases and their animal models. Briefings in Functional Genomics **10:** 258-265, 2011

50 Sellers RS: The gene or not the gene--that is the question: understanding the genetically engineered mouse phenotype. Vet Pathol **49:** 5-15, 2012

51 Sellers RS, Ward JM: Toward a better understanding of mouse models of disease. Vet Pathol **49:** 4, 2012

52 Shuangshoti S, Rushing EJ, Mena H, Olsen C, Sandberg GD: Supratentorial extraventricular ependymal neoplasms: a clinicopathologic study of 32 patients. Cancer **103:** 2598-2605, 2005

53 Shultz LD, Coman DR, Bailey CL, Beamer WG, Sidman CL: "Viable motheaten," a new allele at the motheaten locus. I. Pathology. Am J Pathol **116:** 179-192, 1984

54 Sills RC, Boorman GA, Neal JE, Hong HL, Devereux TR: Mutations in ras genes in experimental tumours of rodents. IARC Sci Publ**:** 55-86, 1999

55 Sills RC, Hong HL, Melnick RL, Boorman GA, Devereux TR: High frequency of codon 61 K-ras A-->T transversions in lung and Harderian gland neoplasms of B6C3F1 mice exposed to chloroprene (2-chloro-1,3-butadiene) for 2 years, and comparisons with the structurally related chemicals isoprene and 1,3-butadiene. Carcinogenesis **20:** 657-662, 1999

56 Simpson EM, Linder CC, Sargent EE, Davisson MT, Mobraaten LE, Sharp JJ: Genetic variation among 129 substrains and its importance for targeted mutagenesis in mice. Nat Genet **16:** 19-27, 1997

57 Smith RS, Montagutelli X, Sundberg JP: Ulcerative blepharitis in aging inbred mice. *In*: Pathobiology of the Aging Mouse, eds. Mohr U, Dungworth DL, Capen CC, Carlton WW, Sundberg JP, Ward JM, pp. 131-138. ILSI Press, Washington, D.C, 1996

58 Suhalim JL, Parfitt GJ, Xie Y, De Paiva CS, Pflugfelder SC, Shah TN, Potma EO, Brown DJ, Jester JV: Effect of desiccating stress on mouse meibomian gland function. Ocul Surf **12:** 59-68, 2014

59 Sundberg JP, Berndt A, Sundberg BA, Silva KA, Kennedy V, Bronson R, Yuan R, Paigen B, Harrison D, Schofield PN: The mouse as a model for understanding chronic diseases of aging: the histopathologic basis of aging in inbred mice. Pathobiol Aging Age Relat Dis **1**, 2011

60 Sundberg JP, Brown KS, Bates R, Cunliffe-Beamer TL, Bedigian H: Suppurative conjunctivitis and ulcerative blepharitis in 129/J mice. Lab Anim Sci **41:** 516-518, 1991

61 Tabata N, Miyazawa M, Fujisawa R, Takei YA, Abe H, Hashimoto K: Establishment of monoclonal anti-retroviral gp70 autoantibodies from MRL/lpr lupus mice and induction of glomerular gp70 deposition and pathology by transfer into non-autoimmune mice. J Virol **74:** 4116-4126, 2000

62 Tanaka T, Rivenson A: Mastocytoma induced by cigarette smoke particulates: "cigarette tar". Arch Dermatol Res **279:** 130-135, 1986

63 Threadgill DW, Matin A, Yee D, Carrasquillo MM, Henry KR, Rollins KG, Nadeau JH, Magnuson T: SSLPs to map genetic differences between the 129 inbred strains and closed-colony, random-bred CD-1 mice. Mamm Genome **8:** 441-442, 1997

64 Threadgill DW, Yee D, Matin A, Nadeau JH, Magnuson T: Genealogy of the 129 inbred strains: 129/SvJ is a contaminated inbred strain. Mamm Genome **8:** 390-393, 1997

65 Vege KD, Giannini C, Scheithauer BW: The immunophenotype of ependymomas. Appl Immunohistochem Mol Morphol **8:** 25-31, 2000

66 Wancket LM, Devor-Henneman D, Ward JM: Fibro-osseous (FOL) and degenerative joint lesions in female outbred NIH Black Swiss mice. Toxicol Pathol **36:** 362-365, 2008

865 67 Ward JM: Pulmonary pathology of the motheaten mouse. Vet Pathol **15:** 170-178,
866 1978
867 68 Ward JM, Anver MR, Mahler JF, Devor-Henneman DE: Pathology of mice
868 commonly used in genetic engineering (C57BL/6; 129; B6,129; and FVB/N).
869 Pathology of Genetically Engineered Mice**:** 161-179, 2000
870 69 Ward JM, Yoon M, Anver MR, Haines DC, Kudo G, Gonzalez FJ, Kimura S:
871 Hyalinosis and Ym1/Ym2 gene expression in the stomach and respiratory tract
872 of 129S4/SvJae and wild-type and CYP1A2-null B6,129 mice. American Journal
873 of Pathology **158:** 323-332, 2001
874 70 Woolford L, de Lahunta A, Baiker K, Dobson E, Summers BA: Ventricular and
875 extraventricular ependymal tumors in 18 cats. Vet Pathol **50:** 243-251, 2013
876 71 Yuan R, Peters LL, Paigen B: Mice as a mammalian model for research on the
877 genetics of aging. ILAR J **52:** 4-15, 2011
878
879

Tables

Table 1. Prevalence of the main categories of clinical signs/abnormalities in aging male and female 129S6/SvEvTac mice as recorded during the last physical examination before euthanasia or spontaneous animal death. Results are reported as no. of affected mice/total no. of examined mice (%).

Main categories of clinical abnormalities	Males	Females
Ocular[a]	33/44 (75%)	12/18 (67%)
Perineal/genital region[b]	17/44 (39%)	9/18 (50%)
Skin[c]	18/44 (41%)	9/18 (50%)
Abdominal distension/enlargment	15/44 (32%)	12/18 (67%)
Locomotor impairment[d]	7/44 (16%)	1/18 (6%)
Hyporesponsiveness to stimuli	26/44 (59%)	11/18 (61%)
Slow or labored respiration	16/44 (36%)	9/18 (50%)
Poor body conditions/emaciation	23/44 (52%)	10/18 (56%)
Hunched posture	17/44 (39%)	6/18 (34%)
External mass(es) [e]	5/44 (11%)	5/18 (28%)

[a]Ocular abnormalities include the following clinical findings: eye discharge, eye opacity, crusting, and/or ulceration of the eyelids and exophthalmos.

[b]Abnormalities of the perineal and/or genital region include the following clinical findings: discharge form the orifices, enlargement/swelling or mass affecting the area, prolapses from the orifices, crusting, and/or ulceration of the area.

[c]Abnormalities of the skin include the following clinical findings: alopecia, scaling, crusting, ulceration, and matted fur.

[d]Locomotor impairment include the following clinical findings: generalized tremors/convulsions, paraparesis, and vestibular syndrome.

[e] External mass(es) includes all the externally visible masses not affecting the ocular or perineal/genital region.

Table 2. Prevalence of tumors in aging male and female 129S6/SvEvTac mice. Results are reported as no. of affected mice /total no. of examined mice (%).

Neoplasms	Males	Females
Adrenal gland		
Adenoma, cortical	1/44 (2%)	0/18 (0%)
Brain		
Ependymoma, malignant	3/44 (7%)	0/18 (0%)
Duodenum		
Adenoma	1/44 (2%)	0/18 (0%)
Harderian gland		
Adenoma, unilateral	11/44 (25%)	1/18 (6%)
Adenoma, bilateral	5/44 (11%)	1/18 (6%)
Adenocarcinoma, unilateral	6/44 (14%)	4/18 (22%)
Adenocarcinoma, bilateral	2/44 (5%)	0/18 (0%)
Hematopoietic system		
Lymphoma	4/44 (9%)	1/18 (6%)
Histiocytic sarcoma	1/44 (2%)	1/18 (6%)
Mast cell sarcoma	1/44 (2%)	0/18 (0%)
Liver		

Neoplasms	Males	Females
Adenoma, hepatocellular	9/44 (21%)	3/18 (17%)
Carcinoma, hepatocellular	6/44 (14%)	0/18 (0%)
Mammary gland		
Adenoma	n/a	1/18 (6%)
Lung		
Adenoma	12/44 (27%)	8/18 (44%)
Adenocarcinoma	6/44 (14%)	3/18 (17%)
Pituitary gland		
Adenoma, pars distalis	0/44 (0%)	1/18 (6%)
Skin		
Hemangiosarcoma	0/44 (0%)	1/18 (6%)
Squamous Cell Carcinoma	0/44 (0%)	1/18 (6%)
Stomach		
Adenocarcinoma	1/44 (2%)	0/18 (0%)
Testis / Abdominal cavity		
Anaplastic malignant tumour	1/44 (2%)	n/a
Uterus		
Adenocarcinoma, endometrial	n/a	1/18 (6%)
Sarcoma, endometrial stroma	n/a	3/18 (17%)
Hemangioma	n/a	1/18 (6%)
Leiomyoma	n/a	1/18 (6%)
Total tumors	77	32
Total benign tumors	44	17

Neoplasms	Males	Females
Total malignant tumors	33	15
Total metastatic/systemic tumors[a]	7	3

n/a, not applicable

[a] these include hematopoietic tumors with multisystemic involvement

900

901 Table 3. Prevalence of non-neoplastic lesions in aging 129S6/SvEvTac mice. For
902 each listed organ/tissue the prevalence of microscopic changes is reported as no. of
903 affected mice/total no. of examined mice (%).

Organ/tissue and lesion	Males	Females
Bones and joints		
Fibro-osseous lesion***	1/43 (2%)	8/17 (47%)
Intervertebral disk degeneration	9/43 (21%)	5/17 (29%)
Intervertebral disk herniation	3/43 (7%)	0/17 (0%)
Bone marrow		
Hemosiderosis	4/44 (9%)	1/17 (6%)
Hyperplasia, erythroid/megakaryocytic	1/44 (2%)	0/17 (0%)
Hyperplasia, myeloid/granulocytic*	3/44 (7%)	6/17 (35%)
Blood vessels (multiple tissues)		
Polyarteritis**	15/44 (34%)	0/18 (0%)
Brain		

Encephalitis, throboembolic with bacteria	1/44 (2%)	0/18 (0%)
Gliosis, not otherwise specified	0/44 (0%)	1/18 (6%)
Inflammatory cell infiltrates/foci, perivascular	0/44 (0%)	1/18 (6%)
Melanosis, meninges	0/44 (0%)	1/18 (6%)
Mineralization, thalamus	4/44 (9%)	2/18 (11%)
Epididymis		
Fibrosis	1/39 (3%)	n/a
Inflammatory cell infiltrates/foci, interstitial	5/39 (13%)	n/a
Pigment accumulation, lipofuscin	2/39 (5%)	n/a
Sperm granuloma	1/39 (3%)	n/a
Sperm stasis	8/39 (21%)	n/a
Esophagus		
Megaesophagus	7/44 (16%)	4/18 (22%)
Eyes and eyelids		
Blepharitis/blepharoconjunctivitis[a,b]	38/42 (91%)	15/16 (94%)
Keratitis[c]	2/42 (5%)	0/16 (0%)
Lens degeneration/cataract	0/42 (0%)	1/16 (6%)
Retinal detachment	1/42 (2%)	1/16 (6%)
Forestomach		
Erosion/ulceration, mucosal	2/44 (5%)	0/18 (0%)
Hyperkeratosis/hyperplasia, mucosal	7/44 (16%)	1/18 (6%)

Inflammatory cell infiltrates/foci, lamina propria/submucosa	1/44 (2%)	0/18 (0%)
Gallbladder		
Hyperplasia with hyalinosis, epithelium	1/30 (3%)	1/12 (8%)
Glandular stomach		
Erosion/ulceration, mucosal	4/44 (9%)	3/18 (17%)
Hyperplasia polypoid, mucosal	1/44 (2%)	0/17 (0%)
Hyperplasia with hyalinosis, mucosal	4/44 (9%)	4/18 (22%)
Hyperplasia with intestinal metaplasia, mucosal	6/44 (14%)	5/18 (28%)
Inflammatory cell infiltrates/foci, lamina propria/submucosa	3/44 (7%)	0/18 (0%)
Yeasts	1/44 (2%)	0/18 (0%)
Harderian gland		
Hyperplasia	5/42 (12%)	3/16 (19%)
Inflammatory cell infiltrates/foci, interstitial	7/42 (17%)	3/16 (19%)
Heart		
Cardiomyopathy	25/44 (57%)	8/18 (44%)
Endocarditis, valvular with bacteria	2/44 (5%)	0/18 (0%)
Fibrosis, pericardial	0/44 (0%)	1/18 (6%)
Inflammatory cell infiltrates/foci, myocardial/epicardial	2/44 (5%)	2/18 (11%)
Melanosis, subendocardial	0/44 (0%)	1/18 (6%)
Mineralization, myocardial	3/44 (7%)	0/18 (0%)

Necrosis, myocardial	1/44 (2%)	2/18 (11%)
Pancarditis, suppurative with bacteria	2/44 (5%)	2/18 (11%)
Kidneys		
Atrophy, tubular	3/43 (7%)	0/18 (0%)
Chronic nephropathy	3/43 (7%)	0/18 (0%)
Cysts, tubular	3/43 (7%)	0/18 (0%)
Degeneration/necrosis, tubular	6/43 (14%)	0/18 (0%)
Dilation/eosinophilic casts, tubular	13/43 (30%)	3/18 (17%)
Glomerulonephritis	3/43 (7%)	0/18 (0%)
Glomerulosclerosis	2/43 (5%)	0/18 (0%)
Hyaline droplets, tubular	1/43 (2%)	0/18 (0%)
Hydronephrosis[d]	8/43 (19%)	6/18 (33%)
Hyperplasia with hyalinosis, pelvic transitional epithelium	0/43 (0%)	2/18 (11%)
Infarcts, cortical	3/43 (7%)	0/18 (0%)
Inflammatory cell infiltrates/foci, interstitial/perivascular	22/43 (51%)	13/18 (72%)
Nephritis, suppurative with bacteria/bacterial emboli	5/43 (12%)	2/18 (11%)
Pyelitis	0/43 (0%)	2/18 (11%)
Large intestine		
Inflammatory cell infiltrates/foci, lamina propria/submucosa	1/44 (2%)	0/18 (0%)
Pinworm nematodes	5/44 (11%)	5/18 (28%)
Liver		

Angiectasis	3/44 (7%)	2/18 (11%)
Degeneration, hepatocellular	11/44 (25%)	2/18 (11%)
Extramedullary hematopoiesis***	4/44 (9%)	12/18 (67%)
Fibrosis	0/44 (0%)	1/18 (6%)
Focus of cellular alteration, hepatocellular	1/44 (2%)	0/18 (0%)
Hyperplasia with hyalinosis, bile duct	3/44 (7%)	3/18 (17%)
Hyperplasia, sinusoidal lining cells	1/44 (2%)	0/18 (0%)
Inflammatory cell infiltrates/foci, portal/intralobular/centrilobular	19/44 (43%)	7/18 (39%)
Karyocytomegaly, hepatocellular	6/44 (14%)	0/18 (0%)
Lobe torsion with infarction	1/44 (2%)	0/18 (0%)
Necrosis, hepatocellular	2/44 (5%)	3/18 (17%)
Regenerative hyperplasia, hepatocellular	3/44 (7%)	2/18 (11%)
Thrombosis/hemorrhage	2/44 (5%)	0/18 (0%)
Lungs		
Eosinophilic Crystalline Pneumonia	26/44 (59%)	11/18 (61%)
Eosinophilic crystals, bronchial/alveolar	30/44 (68%)	13/18 (72%)
Hemorrhage	1/44 (2%)	0/18 (0%)
Inflammation, suppurative	1/44 (2%)	1/18 (6%)

Inflammatory cell infiltrates/foci, perivascular/peribronchial	5/44 (11%)	3/18 (17%)
Thrombosis/necrosis	0/44 (0%)	1/18 (6%)
Lymph nodes		
Depletion, lymphoid	8/32 (25%)	3/13 (23%)
Extramedullary hematopoiesis, increased	0/32 (0%)	2/13 (15%)
Hemosiderosis	8/32 (25%)	0/13 (0%)
Hyperplasia, lymphoid	9/32 (28%)	3/13 (23%)
lymphadenitis	3/32 (9%)	2/13 (15%)
Plasmacytosis*	6/32 (19%)	8/13 (62%)
Sinus dilation	3/32 (9%)	0/13 (0%)
Sinus histiocytosis	12/32 (38%)	4/13 (31%)
Mammary gland		
Galactocele	n/a	3/15 (20%)
Inflammatory cell infiltrates/foci, perivascular/periductal	n/a	1/15 (7%)
Ovary		
Atrophy	n/a	4/8 (50%)
Cyst	n/a	5/8 (63%)
Hematocyst	n/a	3/8 (38%)
Hyperplasia, tubulostromal	n/a	1/8 (13%)
Inflammatory cell infiltrates/foci, stroma/mesovarium	n/a	5/8 (63%)
Pancreas		

Atrophy, exocrine compartment	1/44 (2%)	0/18 (0%)
Cyst, ductal	0/44 (0%)	2/18 (11%)
Fibrosis	0/44 (0%)	1/18 (6%)
Hyperplasia with hyalinosis, ductal	1/44 (2%)	0/18 (0%)
Inflammatory cell infiltrates/foci, interstitial	2/44 (5%)	1/18 (6%)
Preputial gland		
Adenitis, suppurative[e]	10/44 (23%)	n/a
Prostate		
Dilation, acinar	3/7 (43%)	n/a
Inflammation, suppurative	1/7 (14%)	n/a
Skeletal muscle		
Degeneration, myofiber	1/43 (2%)	0/18 (0%)
Fibrosis	1/43 (2%)	0/18 (0%)
Inflammation, suppurative (abscess)	2/43 (5%)	0/18 (0%)
Small intestine		
Amyloidosis	1/44 (2%)	0/18 (0%)
Enteritis, suppurative and/or ulcerative	2/44 (5%)	0/18 (0%)
Inflammatory cell infiltrates/foci, lamina propria/submucosa	3/44 (7%)	1/18 (6%)
Spinal cord		
Spinal cord, hemorrage	0/44 (0%)	1/18 (6%)
Spleen		
Depletion, lymphoid	9/43 (21%)	8/18 (44%)

Extramedullary hematopoiesis, increased***	2/43 (5%)	8/18 (44%)
Hemosiderosis	5/43 (12%)	3/18 (17%)
Hyperplasia, lymphoid	0/43 (0%)	1/18 (6%)
Plasmacytosis	2/43 (5%)	3/18 (17%)
Seminal vesicles		
Dilation	11/14 (79%)	n/a
Inflammation, suppurative[f]	7/14 (50%)	n/a
Torsion/hemorrhage	1/14 (7%)	n/a
Skin		
Abscess, subcutis/fascia	1/35 (3%)	0/15 (0%)
Atrophy, adnexal	1/35 (3%)	3/15 (20%)
Dermatitis chronic with acanthosis and hyperkeratosis[g]	9/35 (26%)	6/15 (40%)
Dermatophytosis	1/35 (3%)	0/15 (0%)
Hematoma, subcutis	1/35 (3%)	0/15 (0%)
Inflammatory cell infiltrates/foci, dermis	4/35 (11%)	3/15 (20%)
Mites	8/35 (23%)	5/15 (33%)
Panniculitis	1/35 (3%)	0/15 (0%)
Squamous epithelial cyst	1/35 (3%)	0/15 (0%)
Ulceration	0/35 (0%)	1/15 (7%)
Testes		
Atrophy, seminiferous tubules	4/39 (10%)	n/a
Necrosis, seminiferous tubules	1/39 (3%)	n/a
Pigment accumulation, lipofuscin	1/39 (3%)	n/a

Urinary bladder		
Cystitis, lymphofollicular*	0/8 (0%)	3/4 (75%)
Cystitis, necrosuppurative with bacteria	0/8 (0%)	1/4 (25%)
Proteinaceous plug	2/8 (25%)	0/4 (0%)
Uterus		
Adenomyosis	n/a	2/17 (12%)
Angiectasis/thrombosis	n/a	9/17 (53%)
Hyperplasia endometrial cystic	n/a	12/17 (71%)
Metritis/pyometra[h]	n/a	8/17 (47%)

n/a, not applicable

[a] in 19 males and 11 females Gram positive rods were observed in association with this lesion

[b] lesion occurred bilaterally in 31 males and 15 females

[c] lesion occurred bilaterally in 1 male

[d] lesion occurred bilaterally in 1 male and 1 female

[e] intralesional bacteria were observed in 5 cases; the lesion was complicated by cellulitis in 4 cases

[f] Intralesional bacteria were observed in 4 cases; the lesion was complicated by peritonitis in 1 case

[g] pustular lesions with intralesional bacteria were observed in 3 cases

[h] Intralesional bacteria were observed in 4 cases, the lesion was complicated by peritonitis in 4 case

*p<0.05; **p<0.01; ***p<0.001 (difference between males and females)

Table 4. Major Contributing Causes of Death (CCOD) in aging male and female 129S6/SvEvTac mice. Results are presented as no. of affected mice/total no. of examined mice (%).

Major Contributory Causes of Death (CCOD)	Males	Females
Neoplastic causes		
Hematopoietic	5/44 (11%)	1/18 (6%)
Harderian gland	0/44 (0%)	1/18 (6%)
Gastrointestinal	2/44 (5%)	0/18 (0%)
Liver	2/44 (5%)	0/18 (0%)
Vascular	0/44 (0%)	1/18 (6%)
Pituitary	0/44 (0%)	1/18 (6%)
Other malignant metastatic tumor	1/44 (2%)	0/18 (0%)
Total	10/44 (23%)	4/18 (22%)
Non-neoplastic causes		
Polyarteritis	5/44 (11%)	0/18 (0%)
Eosinophilic crystalline pneumonia	4/44 (9%)	2/18 (11%)
Megaesophagus	1/44 (2%)	0/18 (0%)
Sepsis	2/44 (5%)	2/18 (11%)
Suppurative metritis/pyometra/peritonitis	n/a	4/18 (22%)
Uterine Angiectasis/thrombosis	n/a	1/18 (6%)
Urologic Syndrome	2/44 (5%)	0/18 (0%)
Necrosuppurative cystitis and hydronephrosis	0/44 (0%)	1/18 (6%)
Seminal vesicle suppurative adenitis	1/44 (2%)	n/a

Major Contributory Causes of Death (CCOD)	Males	Females
Total	15/44 (34%)	10/18 (56%)
Multiple causes or co-morbidities		
Multiple concurrent non-neoplastic causes	10/44 (23%)	2/18 (11%)
Concurrent neoplastic and non-neoplastic causes	7/44 (16%)	3/18 (17%)
Total	17 (39%)	5 (28%)
Undetermined CCOD	2/44 (5%)	0/18 (0%)

n/a, not applicable

Figures

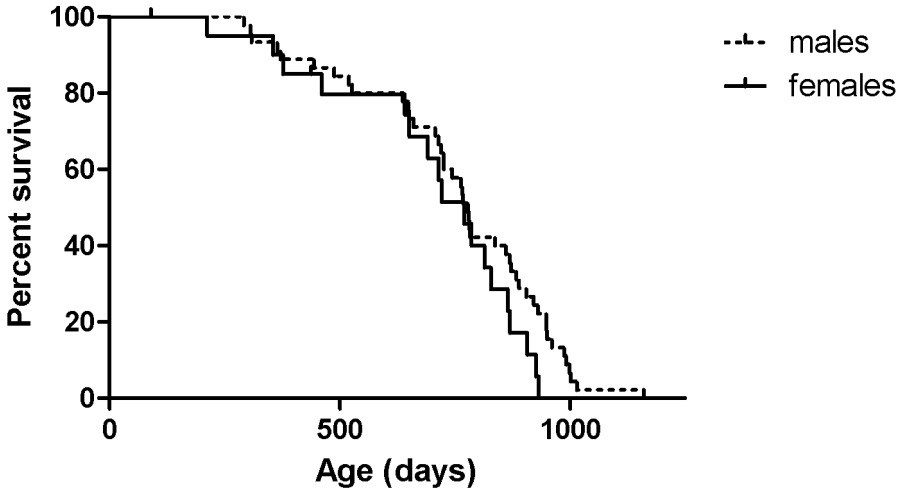

Figure 1. Longitudinal survival study conducted on 129S6/SvEvTac mice. Kaplan-Meier survival curves obtained from 44 males and 18 females.

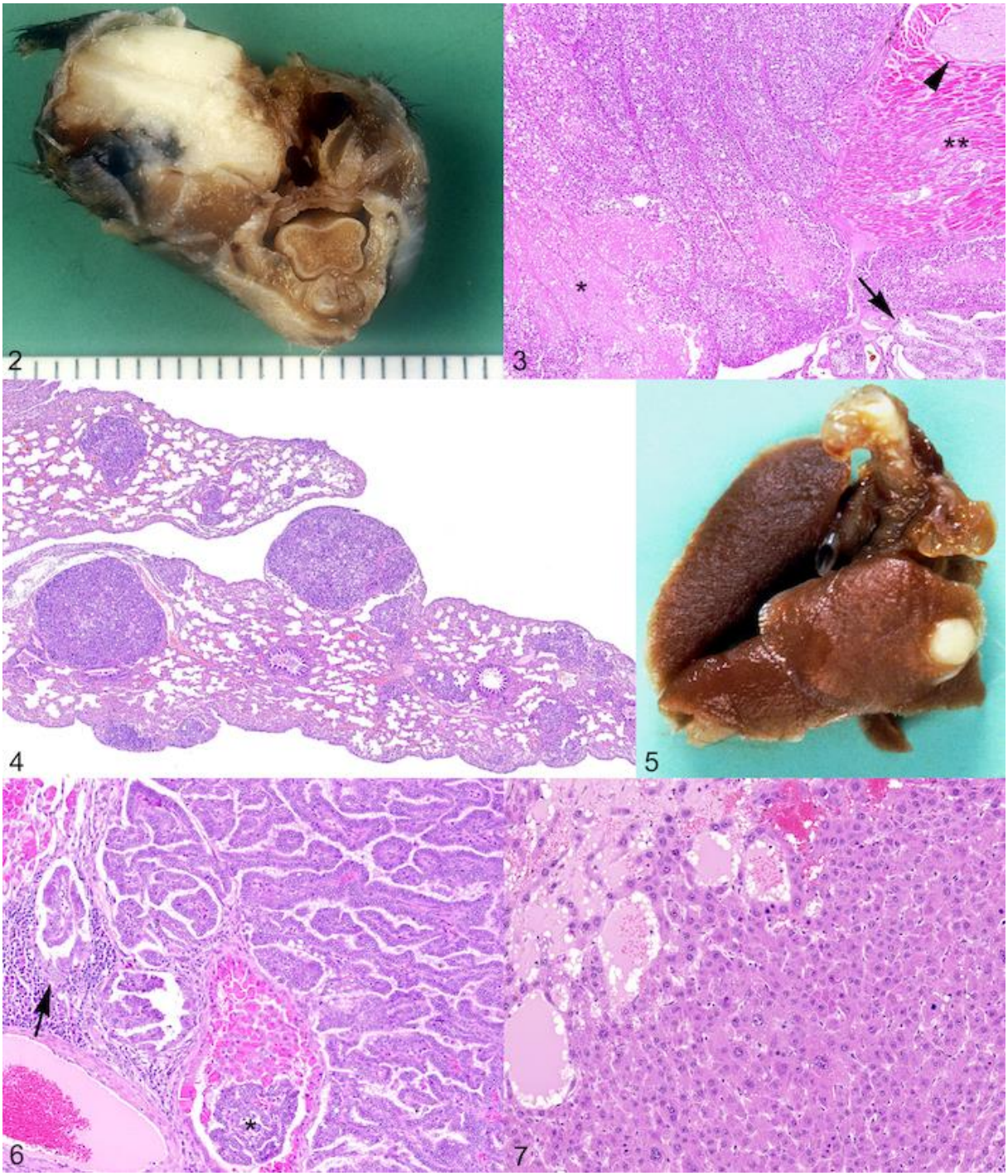

Figures 2-7. Major neoplastic lesions affecting 129S6/SvEvTac mice.

Figure 2. Unilateral carcinoma, Harderian gland, female mouse. Grossly, the tumor exhibits an aggressive growth with local invasion of orbital and periorbital craniofacial structures.

Figure 3. Unilateral Harderian gland carcinoma, female mouse. Microscopically the epithelial neoplasm is arranged in solid densely cellular lobules separated by a delicate

stroma and accompanied by extensive necrotic areas (asterisk). Note the residual orbital structures including Harderian gland (arrow), optic nerve (arrowhead) and extraocular muscles (double asterisk). Hematoxylin and eosin stain.

Figure 4. Harderian gland carcinoma, pulmonary metastases, female mouse. The pulmonary parenchyma is severely affected with disseminated metastatic lesions. Hematoxylin and eosin stain.

Figure 5. Solitary pulmonary carcinoma, female mouse. Grossly the tumor manifests as a well-demarcated whitish solid mass.

Figure 6. Solitary pulmonary carcinoma, female mouse. Microscopically the tumor displays a micropapillary pattern of growth with progressive invasion of the surrounding pulmonary parenchyma (arrow). Note the bronchial outline (asterisk) partially replaced by the infiltrating neoplastic papillary structures. Hematoxylin and eosin stain.

Figure 7. Hepatocellular carcinoma, male mouse. Microscopically the tumor displays a solid to trabecular pattern of growth. Hematoxylin and eosin stain.

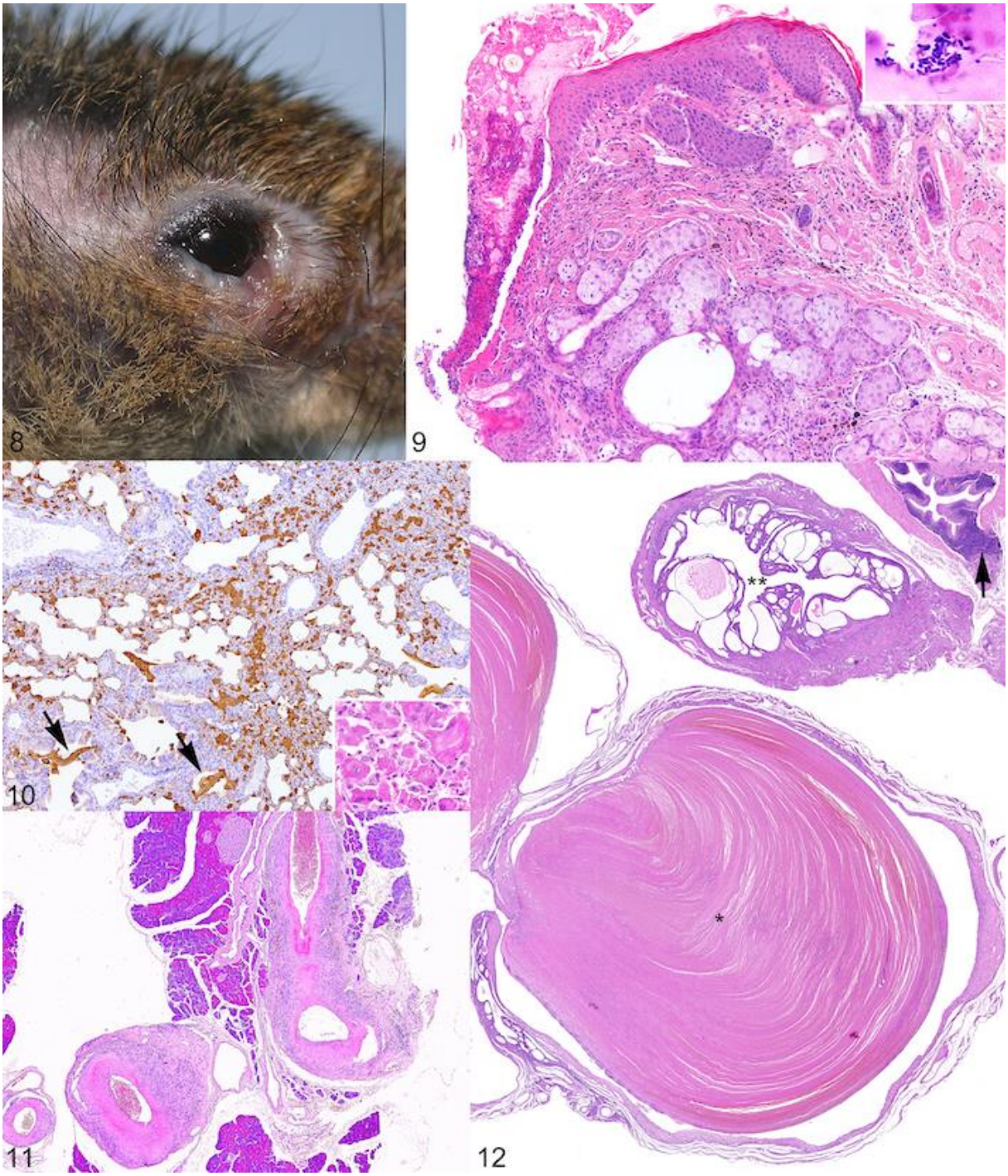

Figures 8-12. Major non-neoplastic lesions affecting 129S6/SvEvTac mice.

Figure 8. Suppurative and ulcerative blepharoconjuctivitis, male mouse. Grossly the affected eye presents suppurative discharge with severe ulceration of the lower eyelid.

Figure 9. Suppurative and ulcerative blepharoconjuctivitis, male mouse. Microscopically the mucocutaneous junction of the affected eyelid exhibits severe ulceration and chronic suppurative inflammation. Gram stain reveals clusters of curved

rod-shaped bacteria populating the serocellular crusts associated with the ulcerative lesion (inset). Haematoxylin and eosin stain; inset, Gram stain.

Figure 10. Eosinophilic crystalline pneumonia, male mouse. The lesion consists of prominent parenchymal infiltrates of Chi3l3/Ym1-positive macrophages which are characterized by abundant intracytoplasmic accumulation of eosinophilic crystalline material (inset). Scattered in the lumen of bronchioles and alveoli are also groups of large elongated extracellular Chi3l3/Ym1-positive crystals (arrows). Immunohistochemistry for Chi3l3/Ym1 protein; inset, hematoxylin and eosin stain.

Figure 11. Polyarteritis, pancreas, male mouse. Microscopically, affected mid-sized arteries display prominent hypertrophy and fibrinoid necrosis of the tunica media associated with fibrosis and inflammatory cell infiltrates expanding the adventitial layer. Haematoxylin and eosin stain.

Figure 12. Urogenital tract lesions, female mouse. A segment of the uterus displays prominent angiectasis and thrombosis in myometrial/endometrial veins (asterisk). Changes consistent with cystic endometrial hyperplasia are also evident in an adjacent segment of the uterus (double asterisk). Note also a portion of the urinary bladder with dense lymphofollicular infiltrates expanding the submucosa (arrow). Hematoxylin and eosin stain.